The Transient Response Characteristics of Compliant Coating to Pressure Fluctuations

Inwon Lee*, Ho Hwan Chun
Advanced Ship Engineering Research Center, Pusan National University, Busan 609-735, Korea
Jin Kim
Maritime and Ocean Engineering Research Institute, Kordi, Korea

The amplitude and phase lag of surface deformation were determined for a compliant coating under the action of turbulent pressure fluctuations. For this purpose, pressure fluctuations were measured experimentally. The amplitude and duration of coherent wave train of pressure fluctuations were investigated using digital filtration. The transient response was calculated for stabilization of forced oscillations of the coating in approximation of local deformation. The response of coating was analyzed with considerations of its inertial properties and limited duration of coherent harmonics action of pressure fluctuations. It is shown that a compliant coating interacts not with the whole spectrum of pressure fluctuations, but only with a frequency range near the first resonance. According to the analysis, with increasing elasticity modulus of the coating material E, deformation amplitude decreases as $1/E$, and dimensionless velocity of the coating surface decreases as $1/\sqrt{E}$. For sufficiently hard coatings, deformation amplitude becomes smaller than the thickness of viscous sublayer, while surface velocity remains comparable to vertical velocity fluctuations of the flow.

Key Words : Drag Reduction, Compliant Coating, Turbulent Boundary Layer, Unsteady Deformation Analysis

Nomenclature

C : Complex compliance of coating
C_{sh} : Shear wave speed ($C_{sh}=\sqrt{E_{sh}/\rho}$)
C_{st} : Static complex compliance
E : Modulus of elasticity of viscoelastic coating material
E_{sh} : Shear modulus of viscoelastic coating material
f_0 : 1st resonance frequency of coating
H : Thickness of coating
K_d : Amplification factor ($K_d=|\zeta(H, t)|/\Delta_{st}$)
N : Number of periods
U_∞ : Freestream velocity
u_0 : Rms streamwise velocity fluctuation in the rigid-wall turbulent boundary layer
u_τ : Friction velocity ($u_\tau=\sqrt{\tau_w/\rho_0}$)
v_0 : Rms normal velocity fluctuation in the rigid-wall turbulent boundary layer
v_{coat} : Normal component of coating deformation velocity
Δ_{st} : Static deformation of coating ($\Delta_{st}=PH/E$)
η : Loss factor of coating material
λ : Wavelength of coating deformation
Θ : Phase of the coating deformation
ρ : Density of viscoelastic coating material
ρ_0 : Density of fluid
τ_w : Skin friction

* Corresponding Author,
E-mail : inwon@pusan.ac.kr
TEL : +82-51-510-2764; **FAX** : +82-51-581-3718
Advanced Ship Engineering Research Center, Pusan National University, Busan 609-735, Korea. (Manuscript **Received** July 13, 2005; **Revised** February 10, 2006)

ζ : Coating deformation
Ω : Nondimensional frequency

1. Introduction

The study of compliant coating has been a recurrent research topic for nearly 50 years. The history of associated studies can be classified into several stages. The initial, celebrated success by Kramer (1957) inspired many researchers to attempt to reproduce and understand his results. Experimental works were about drag reduction in turbulent flows (Blick and Walters, 1968; Lissaman and Harris, 1969) and about transition delay (Benjamin, 1960). Dixon et al.(1994) reported results of optimizing a two-layer coating, the transition Reynolds number becomes 5 times the value for a rigid surface. In the experiments of Gaster (1988), 30% higher transition Reynolds number was reported in association with the compliant coating.

Kramer's coatings (1960) imitated the dolphin's skin and had very complex structures : several layers of viscoelastic materials connected by columns or ribs and, in addition, filled with viscous liquid. Analysis of oscillation characteristics for these coatings is extremely difficult, having remained unsolved until now. In the first stage of study, simpler coatings, the so-called 'membrane coatings', were used. There are many constructions of compliant coatings and different parameters need to describe its properties. Classification of coatings schemes, taken from Kulik et al. (1991), is given in Fig. 1. The oscillation characteristics of membrane-coatings might change in wide region from the film stresses (in different directions) and using liquids with different viscosity. However, these coatings cannot be used in practice. A critical review of the first stage of study was presented by Bushnell et al.(1977).

An alternative to the membrane coating is the single-layered coating, which consists of homogeneous viscoelastic materials. This type is more practical in terms of construction. According to the relationship between the shear wave speed $C_{sh}=\sqrt{E_{sh}/\rho}$ and the freestream velocity U_∞, the coating is classified into two categories; 'soft' coating, in which a traveling shear wave develops (Gad-El-Hak, 1986; Lee et al., 1993), and 'hard' coating, which 'locally' deforms to the pressure fluctuations (Semenov and Semenova, 1988).

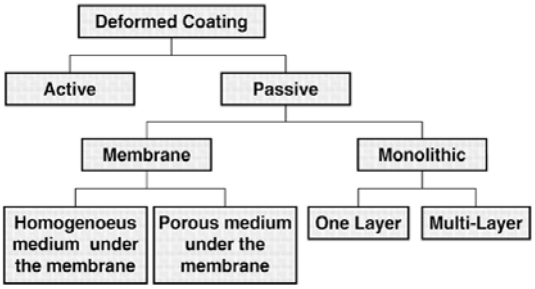

Fig. 1 Classification of compliant coatings

For the 'soft' coating, the condition of the existence of the traveling waves $C_{sh}<U_\infty/1.2$ (Duncan et al., 1985), yields the upper limit for the shear modulus of the coating. This kind of coating should be in a jelly-like state, which is not applicable to real practice. Comprehensive review of theoretical and experimental studies was made by Gad-el-Hak (1996). On the other hand, the 'hard' compliant coating consists of strong enough materials with high modulus of elasticity (Kulik et al., 1991; Choi et al., 1997). Typical hard coatings have been made from silicone rubber with the thickness H varying from 2 to 7 mm and modulus of elasticity E being roughly 5 MPa. The major drawback of this material is the temporal change of viscoelastic properties (aging) (Kulik, 2000).

The drag reduction mechanism by compliant coating was first attributed to the dissipation of turbulent energy inside coating by Kozlov et al. (1985). This attempt, however, lacked the detailed measurement data, especially dynamic viscoelastic material properties. Later it was found that this hypothesis contradicted to the experimental results by Semenov and Semenova (1988). Kulik et al.(1991) also demonstrated that energy dissipation inside the coating is responsible for only 0.01% of the total energy dissipation.

Semenov (1991) suggested and developed a kinematical hypothesis of interaction between compliant coating and turbulent flow, as shown in Fig. 2. Turbulent pressure fluctuations deform the

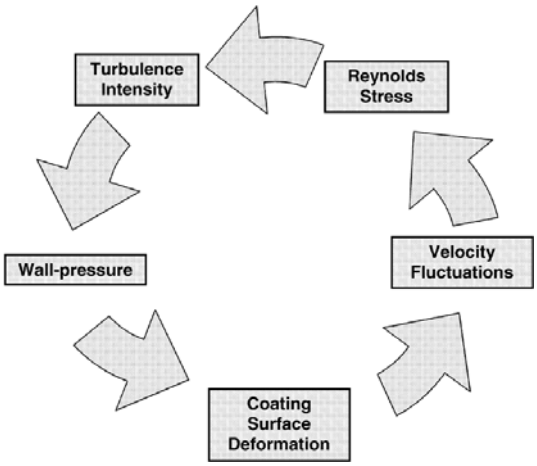

Fig. 2 Mechanism of drag reduction by compliant coating

coating surface. In the near-wall region the disturbances from coating are added to the velocity fluctuations, thereby changing the Reynolds stress. When the change is such that the turbulence production decreases, it eventually leads to drag reduction. Using simple models of turbulence, it was shown that the phase lag of coating deformation from pulsated pressure should be in certain range (Semenov, 1991). This condition was satisfied when the dimensionless resonance frequency $f_0^+=f_0\nu/u_\tau^2$ lies within the range $0.02<f_0^+<0.6$. This condition is consistent with the idea of Fisher et al.(1975) for damping turbulent bursts by coating.

The above-mentioned researches were based on the assumption of 'stationary deformation', which implies an instantaneous interaction of the coating under the action of pressure fluctuations. To be more specific, harmonic interaction with constant amplitude $Ae^{i\omega t}$ is considered in this regime. Figure 3 delineates differences in various assumptions for the analysis of coating deformation. Real compliant coating is characterized with its inertial properties, that is, finite density and nonzero loss tangent. It is apparent that a real compliant coating cannot oscillate instantly, owing to its inertial properties. This implies that the temporal relaxation process of coating deformation under the action of non-stationary pressure fluctuations should be analyzed.

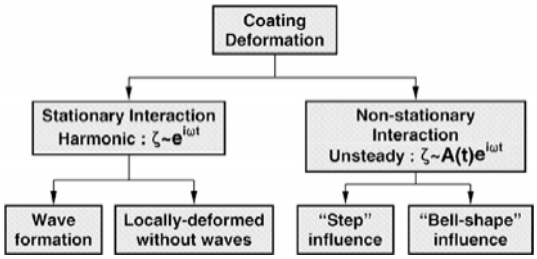

Fig. 3 Classification of assumptions for the analysis coating deformations

In summary, investigations of the response of compliant coating to pressure fluctuations can be separated into characterization of the unsteadiness of pressure fluctuations and analysis of transient coating response. Toward shedding some lights on these two aspects, the present study consists of three parts ; experimental investigation of the unsteady coherent characteristics of wall pressure fluctuations (Section II) and a calculation of coating response for the step-form pressure fluctuations (Section III) and for the bell-shape oscillatory wave-train (Section IV), followed by the discussion on the importance of the loss factor in maximizing compliant coating deformation and hence the drag reduction effect (Section V).

2. Measurements of Duration of Coherent Action of Wall Pressure Harmonics

If the applied pressure fluctuations are completely random, the corresponding coating deformation becomes very small due to the inertia effect. To effectively "excite" the coating, the applied load should be coherent over for a certain period of time. If the duration of such coherent impact is short, the amplitude at the end of the action will be lower than that for the case of stationary impact with the same force. It will be investigated in the later section how deformation amplitude depends upon the impact frequency and duration. The duration of coherent action of pressure fluctuations is also experimentally determined in this section for the case of hydrodynamic measurements in an open channel with

natural external turbulence (Kulik et al., 1991).

The wall-pressure signatures caused by the convecting turbulent eddies were analyzed by Russell (1998). When the vortex structure passes by the pressure transducer, the narrow-band analyzer yields an output signal, the envelope of which has a dome-like shape. As this structure approaches the sensor, the harmonic amplitude will first increases, and then decay out (Fig. 4). Pressure fluctuations filtered by a narrow-bandpass filter have a quasi-coherent character during the whole period of a vortex structure passing by the probe, that is, the period of one wave train. Therefore, the time of coherent impact is determined by duration of a wave train.

Recording of the pressure fluctuation signal was performed using a measurement recorder (Schlumberger) with frequency modulation. The diameter D of the sensing area of the transducer was $D \approx 1.5$ mm. This probe was flush-mounted to the streamlined surface of a body of revolution towed at a velocity of 9 m/s, within zero pressure gradient turbulent flow. Details of the measurement setup can be found in Kulik et al. (1991) and Choi et al.(1997). Digital filtering of a signal was performed using a specially developed software package. The standard soundboard "Vibra 16" was used for the data acquisition. The signal was quantized under the 16-bit mode at three sampling frequencies : 11,025, 22, 050, 44,100 Hz. Bandpass filtering was performed using a pulse filter with finite response region with the Potter window. The bandwidths of the filter were set to four regimes : octave, 1/3-octave, 1/6-octave, and 1/9-octave. The passband ripple, the nonuniformity inside the passband, is almost negligible and the decay rate beyond the passband is over −110dB/octave.

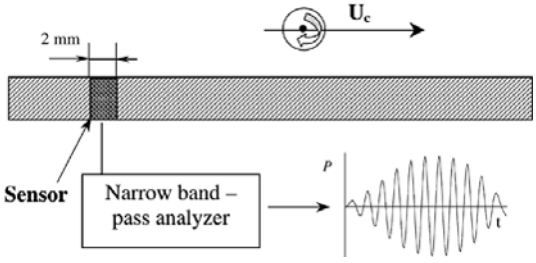

Fig. 4 The measurement scheme

Typical signals after filtering are shown in Figs. 5 and 6. The filtered pressure signal largely

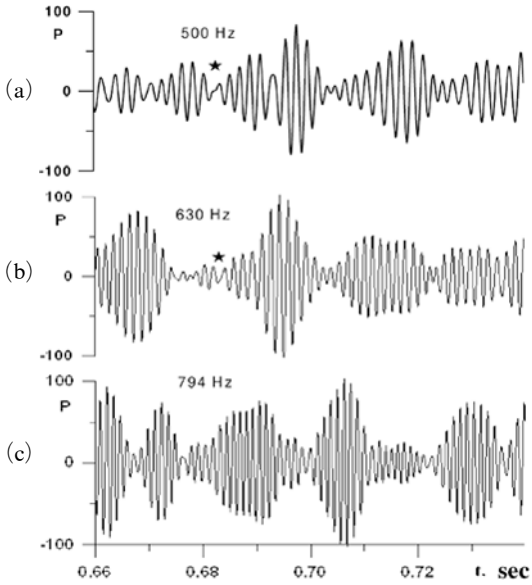

Fig. 5 Filtered pressure signal examples using 1/3-octave filters with varying center frequency f_0 : (a) f_0=500 ; (b) f_0=630 ; (c) f_0=794 Hz

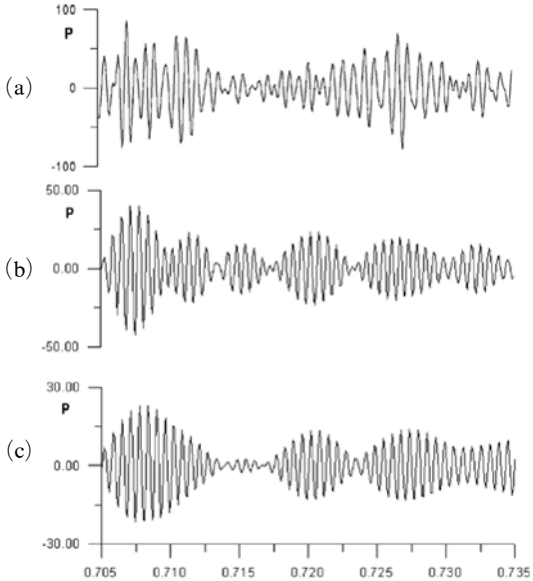

Fig. 6 Filtered pressure signal examples with the center frequency f_0=1587 Hz and varying bandwidth, (a) octave filter ; (b) 1/3-octave filter ; (c) 1/6-octave filter

consists of two parts ; one is fundamental oscillation component corresponding to the center frequency of the filter and the other is low-frequency modulation component representing the envelope. The shape of envelope is largely asymmetric with time, while symmetric is found only occasionally (e.g. Fig. 5(c) at $t=0.722-0.736$ sec ; Fig. 6(b) and (c) at $t=0.717-0.723$ sec). With 1/3-octave bandpass filtering (in Fig. 5), visual separation of the oscillation trains becomes possible from intermediate filter frequency of $f_0>500$ Hz. With increasing center frequency, it is necessary to use filters with narrower bandwidth. Thus, at the frequency of $f_0=1587$ Hz (Fig. 6), octave filtering is not efficient, while the 1/6-octave filter does not provide additional information in comparison with the 1/3-octave filter.

In order to describe the response of a compliant coating to turbulent pressure fluctuations, it is important to know the characteristics of coherent impact, that is, the shape of the wave-train envelope and the number of oscillations in one wave train. It is found that a change in oscillation phase occurs at the wave-train boundaries, as marked by stars in Fig. 5. It is notable that the duration of quasi-coherent action may be longer than one train of oscillations.

Closer comparison of the wave trains reveals the similarity that one wave-train consists of several oscillations, the number of which increases from 5 (at a frequency of 600 Hz) to 10 (1.5 kHz) with increasing filter frequency. This is because the vortical structure, consisting of various scales and frequency components, moves as a whole with a fixed convective velocity. For comparison, based on the measurement of Willmarth (1975), Duncan (1986) assumed for his calculations that there are six oscillation periods in one wave train.

3. Calculation of a Transition Regime for Stabilization of Forced Oscillations

A transitional regime for the stabilization of forced oscillations is investigated in the current section for the simplest coating consisting of a single layer of homogeneous viscoelastic material glued to a solid substrate. The coating material has an elasticity modulus E and viscosity μ. It is also assumed that coating deforms only locally (Kulik, 2000).

Let $\zeta(y, t)$ be a displacement of coating layer at height y at time t. The equation of coating oscillations takes the following form (Semenov and Semenova 1988 ; Kulik 2000)

$$\rho\frac{\partial^2\zeta}{\partial t^2}=E\frac{\partial^2\zeta}{\partial y^2}+\mu\frac{\partial^3\zeta}{\partial y^2\partial t} \tag{1}$$

with initial conditions

$$\zeta(y, t)=0,\ \frac{\partial\zeta}{\partial t}=0 \text{ at } t\leq 0 \tag{2}$$

and boundary conditions

$$\zeta(y)=0 \text{ at } y=0 \text{ (on a rigid wall)}$$
$$P(t)=-E\frac{\partial\zeta}{\partial y}-\mu\frac{\partial^2\zeta}{\partial y\partial t} \text{ at } y=H \tag{3}$$
(on a flexible surface)

where

$$P(t)=\begin{cases}0 & \text{for } t<0\\ P\exp(i\omega t) & \text{for } t\geq 0\end{cases}$$

Here, P is the amplitude of wall pressure with frequency ω. Using the integral transformation of Laplace, we obtain the following :

$$\zeta(H, t)=\frac{1}{2i\pi}\int_{-i\infty}^{i\infty}\frac{P\exp(\xi t)}{(\xi-i\omega)\,\xi\sqrt{\rho(E+\mu\xi)}}\tanh\left(\xi H\sqrt{\rho/(E+\mu\xi)}\right)d\xi$$

Singular points are :

1. $\xi=0$;
2. $\xi=i\omega$;
3. $\xi=-E/\mu$;
4. $\xi_k=\dfrac{-\pi^2(2k+1)^2\mu+\pi(2k+1)\sqrt{\pi^2(2k+1)^2\mu^2-16\cdot H^2E\rho}}{8H^2\rho}$

The first special point yields a trivial solution independent of t, the second point yields stabilized oscillations, the third point is the limit case in succession ξ_k as $k\to\infty$. Singular points 4 describe a transient response. Summing all the deductions, we finally get the following :

$$\zeta(H, t) = -\frac{P\exp(i\omega t)}{i\omega\sqrt{(E+i\omega\mu)\rho}}\tanh\left(\frac{i\omega H}{\sqrt{(i\omega\mu+E)/\rho}}\right) - \frac{2P}{H\rho}\sum_{k=-\infty}^{\infty}\frac{\exp(\xi_k t)(\mu\xi_k+E)}{\xi_k(\xi_k-i\omega)(\mu\xi_k+2E)} \quad (4)$$

Using the relationship

$$\sqrt{1+ia} = \frac{1}{\sqrt{2}}(\sqrt{\sqrt{1+a^2}+1} + i\sqrt{\sqrt{1+a^2}-1})$$

after separation of the real and imaginary parts, equation (4) can be arranged in the form of

$$\xi(H, t) = |\zeta(H, t)|\exp[i(\omega t-\Theta)]$$

Viscoelastic properties of real materials generally depend on frequency. At a fixed temperature, there exists a plateau region where the elasticity modulus and loss tangent $\eta=\mu\omega/E$ scarcely depend on frequency.

Figures 7(a) and (b) represent the three-dimensional contour plots of coating deformation amplitude $|\zeta(H, t)|$ and phase Θ as a function of the number of time-periods of oscillation N and a dimensionless frequency Ω, which is defined as

$$\Omega = H\omega\sqrt{\rho/E}\left[\frac{\sqrt{1+\eta^2}+1}{2(1+\eta^2)}\right]^{1/2} \quad (5)$$

For transient response, the number of periods N is meaningful, because it is a measure of time normalized by the period of each frequency component. ($N=t/(2\pi/\omega)=\omega t/\pi$). Under the stable oscillation regime, the coating deformation depends only on the frequency parameter Ω. There is no generalized parameter for describing of the transient regime in contrast to steady oscillations (this will be discussed later), therefore, in Fig. 7 we used coating properties almost similar to those in Kulik et al.(1991) and Choi et al. (1997), namely: $H=5$ mm, $E=5\times10^6$ Pa, $\rho=2\times10^3$ kg/m^3, $\eta=0.2$ and $P=1$ Pa. Here, as shown by Semenov (1996), the amplitude of steady oscillations has several maximums depending on oscillation frequency. The first of them corresponds to the natural resonance at the dimensionless frequency $\Omega_1\approx\pi/2$. With increasing frequency Ω, the amplitude in the transient regime becomes more oscillatory with respect to N, and the steady regime begins from a larger value of N. In addition, the phase

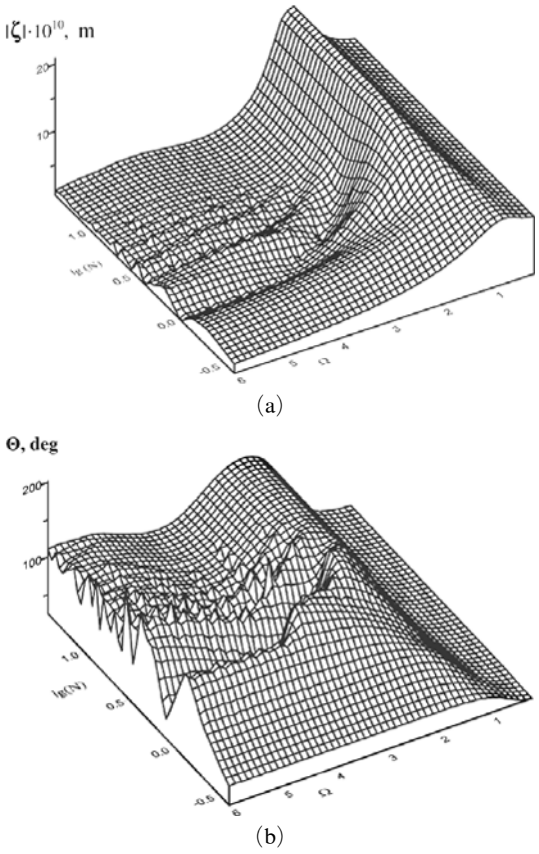

Fig. 7 Contour plots for the transient response of amplitude (a) and phase (b) of forced oscillations

exhibits clearer oscillatory behavior than the amplitude does.

For easy comparison, Fig. 8 illustrates transient processes at the first resonance frequency. The amplification factor $K_d=|\zeta(H, t)|/\Delta_{st}$, deformation amplitude $|\zeta(H, t)|$ normalized by static deformation value $\Delta_{st}=PH/E$, decreases significantly with increasing loss tangent η. Same tendency can be found for the transition time, which is the time required for the amplitude K_d to attain a saturated value. The number of oscillation periods N_l required to reach the given amplitude level $l=|\zeta(t)|/|\zeta(t=\infty)|$ at the frequency of the first resonance is shown in Fig. 9. For $\eta>0.4$, the relaxation time to $l=0.708=1/\sqrt{2}$ becomes less than one oscillation period. To excite the coating to the half of the stationary oscillation levels ($l=0.5$), it takes roughly half

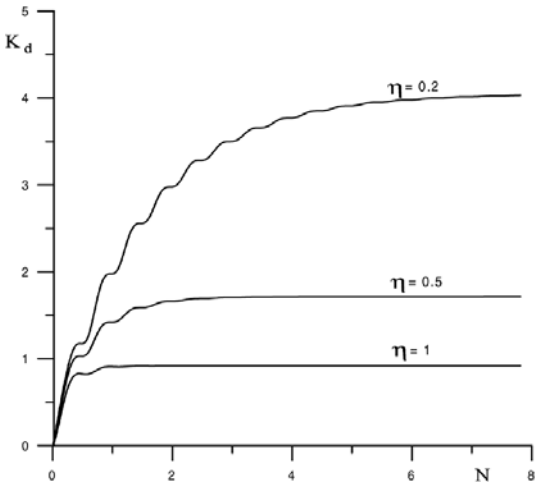

Fig. 8 Transient process for stabilization of amplitude of forced oscillations at the first resonance frequency

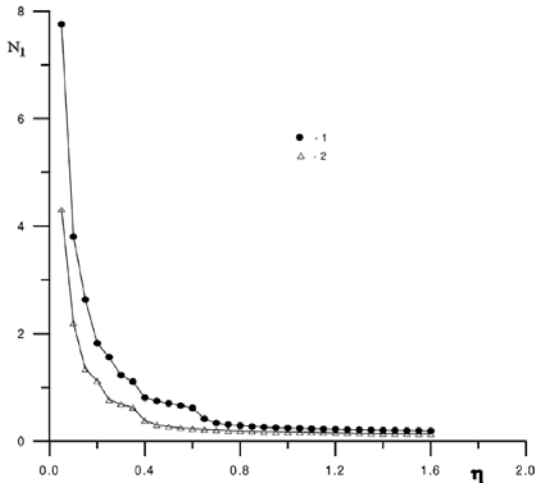

Fig. 9 The number of oscillation periods required to attain the given amplitude level. $l=0.708$ (●), 0.5 (△)

of that required to reach the level $l=0.708$. For materials with a loss-tangent plateau (η does not depend on frequency), change of the coating material parameters (E, ρ and H) leads only to a change in frequency ω of the first resonance and does not affect the relaxation process. Therefore, the relationships obtained are true for the whole range of E, ρ and H.

For the higher order resonance frequencies, analysis revealed a drastic increase in the relaxation time for amplitude and phase. Therefore, while analyzing the interaction between a single-layer viscoelastic coating and a turbulent flow, for most cases, it is sufficient to consider only the first resonance.

4. Response to the Bell-Shape Oscillation Train

As shown in Fig. 8, the rate of rise in oscillation amplitude is very similar for different η in the initial period of relaxation ($N<0.5$), after that for small η, it becomes higher. Therefore, a flexure of the coating surface with $\eta>0.8$, which relaxes during one oscillation period to the level of 0.95, repeats the shape of pressure fluctuations change (the wave-train shape), without resonance. On the other hand, the time of relaxation is longer than one oscillation period for the coatings with a low loss tangent ($\eta<0.5$). Thus, the coating deformation does not simply repeat the shape of pressure fluctuations wave train but becomes dependent upon the previous oscillations cycles.

Coating response to wall pressure, changing as $P(t)=P_{env}\exp(i\omega t)$ was analytically calculated. Frequency ω was chosen equal to the first resonance frequency of the coating. The envelope was approximated by the following exponential functions:

$P_{env}=P_0[1-\exp(-t/\tau)]$ — for regions of growth,
$P_{env}=P_0'\exp(-t/\tau)$ — for regions of attenuation.

The time constant τ of pressure envelope, approximately corresponding to one fourth of the wave-train duration, was chosen to be equal to one, two and three oscillation periods.

The dimensionless velocity of compliant coating surface

$$v_{coat}^{+}=\frac{1}{u_\tau}\frac{\partial\zeta}{\partial t} \tag{6}$$

Flow parameters are the same as those in Section II: $U=9$ m/s, $\tau_w\approx150$ Pa, $u_\tau\approx0.4$ m/s, $P_0\approx300$ Pa, P_0' has been obtained from the condition of smooth joint of the growth envelope and decline envelope.

Fluctuating pressure and response of a compliant coating are shown in Fig. 10 for the case

of growing pressure envelope, as $P_{env}=P_0[1-\exp(-t/\tau)]$ with $\tau=3$ ($T=-2\pi/\omega$ - oscillation period). Both the amplitude and relaxation time of dimensionless velocity of coating oscillation in Fig. 10(b) decreases with the increasing loss tangent η. However, as shown v^+ in Fig. 10 (c), the phase shift between the velocity of coating oscillation and the pressure fluctuations relaxes to constant value of $\Theta\approx160-170°$ during one oscillation period, regardless of the loss tangent η.

Figure 11 illustrates the behavior of a com-

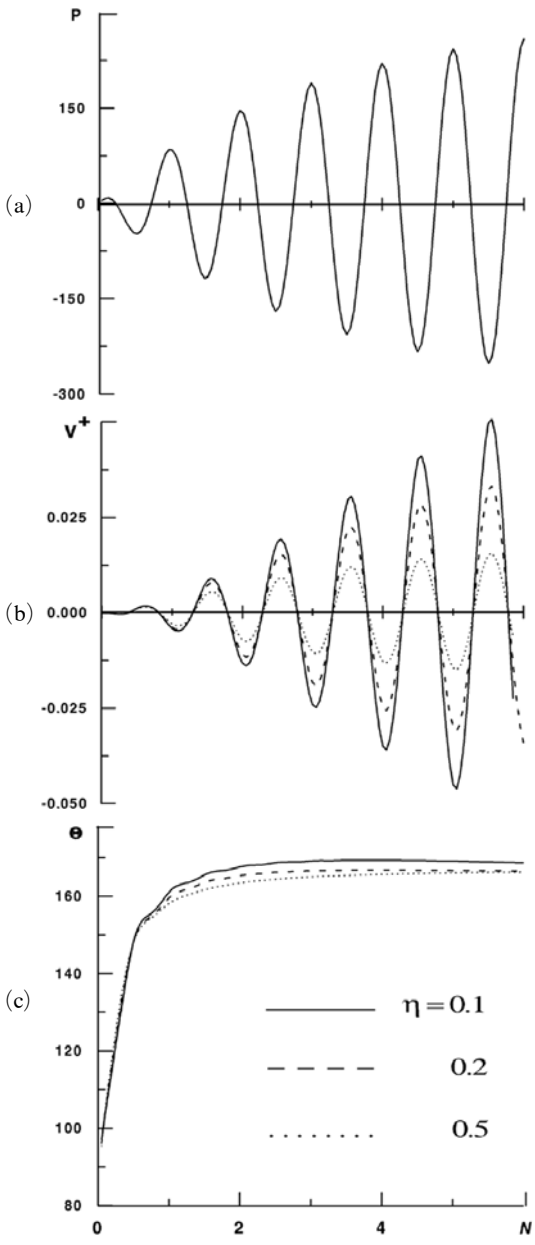

Fig. 10 Response of the coating to pressure fluctuations P changing as $P=P_0(1-\exp(-t/\tau))$, $\tau=3$ oscillation periods. (a) pressure fluctuations; (b) dimensionless velocity of coating surface v^+; (c) phase shift between v^+ and P

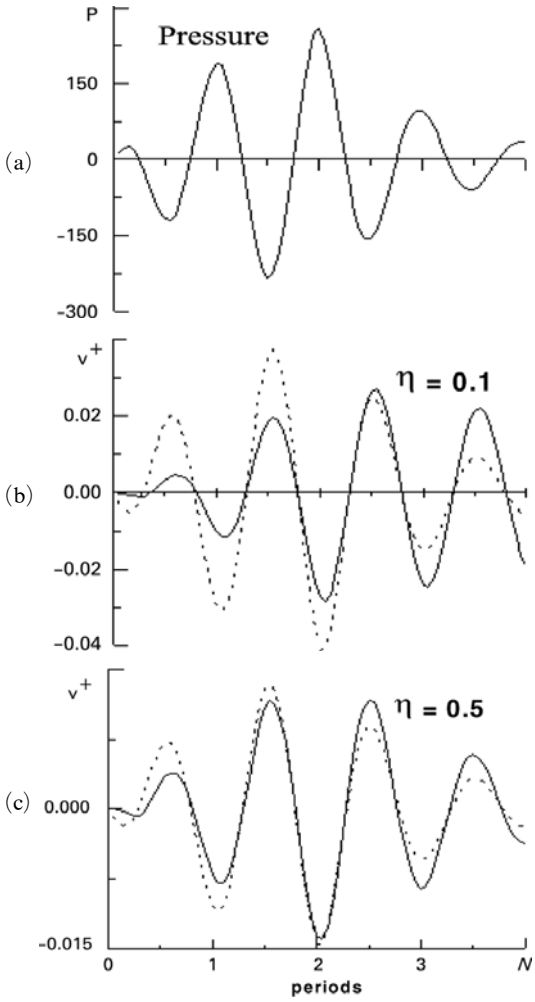

Fig. 11 Response of the coating to pressure fluctuations P changing as $P=P_0(1-\exp(-t/\tau))$ for $0<N<2$ and $P_0\exp(-t/\tau)$ for $2<N<4$, τ is equal to one oscillation period. (a) pressure fluctuations; (b) v^+ for $\eta=0.1$; (c) v^+ for $\eta=0.5$, Dashed curves corresponding to zero relaxation time ($\eta=0$)

pliant coating in the case of the wave train of pressure fluctuations, consisting of four oscillation periods (Fig. 11(a)). At low η in Fig. 11 (b), oscillations of the coating surface rise and decay slowly, and this leads to an asymmetrical shape of deformation wave train. As mentioned above, the dimensionless velocity for the coating with $\eta=0.1$ is almost twice as large as that for the coating with $\eta=0.5$. For comparison, v^+ is shown with a dashed curve for the hypothetical case with zero time of relaxation, that is, the coating deformation being proportional to the pressure fluctuations ($\eta=0$). The case of higher loss tangent $\eta=0.5$ in Fig. 11(c) exhibits a smaller discrepancy with the ideal no inertia coating (i.e., zero relaxation time). Thus, the difference between the 'real' coating deformation and the 'ideal' coating deformation becomes larger with decreasing loss tangent η. It is also noteworthy that within the growth regions, the oscillation amplitude of the real coating is less than that of the ideal coating, and that during the attenuation region, it is higher.

These results demonstrate that the coating almost always operates under the transient regime and never reaches maximal deformation amplitudes typical of the steady regime. This difference increases drastically with a decrease in the number of oscillations in one wave train of pressure fluctuations, namely the decrease in time duration of coherent pressure fluctuations.

5. Discussion

The coating deformation is described in terms of compliance, which is defined as

$$\zeta=C\cdot P$$

where $C-$ is compliance, $P-$ wall pressure. ζ and P is RMS-values. For static deformation $C_{st}=H/E$; but for unsteady coating deformation in a turbulent flow the amplification factor k_d (Semenov, 1996) should be used. For real coatings, the measured k_d values were found to be less than the calculated one ($k_d\approx 1\sim 3$) (Kulik et al., 2005). It would be worthwhile to roughly estimate the coating deformation and velocity magnitude in real cases. Pressure fluctuations in a turbulent flow under a flat plate can be correlated as $P\approx 2.75\tau_w$ (Kraichnan, 1956). For 'hard' compliant coatings ($E=5$ MPa, $\rho=2\times 10^3$ kg/m^3, $H=5\times 10^{-3}$ m) and for $U=10$ m/s, $\tau_w\approx 150$ Pa yields in the optimal stationary regime $\zeta<1.5\times 10^{-6}$ m, which corresponds to $\zeta^+=\zeta u_\tau/v\approx 0.4$, where $\mu_\tau=\sqrt{\tau_w/\rho_0}$ is the friction velocity and ρ_0 is the liquid density. So, the displacement of the coating surface is essentially less then the thickness of laminar sublayer. The normal velocity of coating is calculated as $v_{coat}=2\pi f_0\zeta$, where f_0 is the resonance frequency of a coating $f_0\approx\sqrt{E/\rho}/4H$. In connection with the above case $v^+_{coat}=v_{coat}/u_\tau$, was estimated to be 0.1. It is notable that in the vicinity of the coating (i.e., at $y^+\sim 1$), the rms velocity fluctuations u_0^+, v_0^+ for the 'rigid-wall' turbulent boundary layer were found to be u_0^+, $v_0^+\sim 0.2$ (Spalart, 1988). This implies that the 'rigid-wall' velocity fluctuations are comparable to the velocity of the coating. This also shows that the 'hard' compliant coating can have important influence on Reynolds stresses in near-wall region in spite of the small amplitude of surface deformation.

$$\begin{aligned}\tau_w&\approx\langle(u_0+u_{coat})(v_0+v_{coat})\rangle\\&=\langle u_0u_0\rangle+\langle u_0v_{coat}\rangle+\langle u_{coat}v_0\rangle+\langle u_{coat}v_{coat}\rangle\end{aligned}$$

The dependency of the dimensionless coating velocity on the parameters of compliant coating and of flow is given as

$$\begin{aligned}v^+_{coat,stat}&=\frac{1}{u_t}\frac{\partial\zeta}{\partial t}\\&=\frac{Pe^{i\omega t}}{u_\tau}\frac{i\tanh(i\omega H\sqrt{(\rho/E(1+i\eta)})}{\sqrt{\rho E(1+i\eta)}}\end{aligned}\quad(7)$$

Here P is the amplitude of single harmonic component of wall pressure fluctuations with frequency ω. Among various frequency components, the component with frequency $\Omega_1\approx\pi/2$ (natural resonance of a compliant coating) makes the largest contribution in interaction between a coating and a flow. In practice, the measured quantity is not the amplitude of a separate harmonic, but rather a root-mean-square value of pressure fluctuations in a certain frequency range. Therefore, the value of $v^+_{coat,stat}$ in Eq. (7), will correspond

to the root-mean-square coating velocity in the same frequency range. This is because the linear dependence of deformation on applied pressure holds for very small magnitude of coating deformation (relative deformation $\zeta/H \approx 10^{-4}$). Similarly as the empirical correlation between the root-mean-square value of fluctuating wall pressure in the whole frequency range and the shear stress $P \approx 2.75\tau_w$ (Kraichnan, 1956), for the first resonance frequency component, we can write $P_{rms} = K'_{Kr}\,\tau_w$, where K'_{Kr} is the modified Kraichnan coefficient. Taking into account $\tau_w = \rho u_\tau^2$, we will finally obtain:

$$v^+_{coat,stat} \approx iK'_{Kr}\,\frac{u_\tau}{\sqrt{E/\rho}} \cdot C_{coat} e^{i\omega t} \qquad (8)$$

where $C_{coat} = \tanh\left[i\,\frac{\pi}{2}(1+\eta^2)^{1/4}\Big/\sqrt{1+i\eta}\right]\Big/\sqrt{1+i\eta}$. The value of $\sqrt{E/\rho}$ determines the propagation velocity for perturbations in the coating material. Figure 12 plots the magnitude of C_{coat} as a function the loss tangent. The dependence of $|C_{coat}|$ on the loss tangent can be approximated as $|C_{coat}| \approx 1.472\eta^{-0.914}$. Thus, at the first resonance, the dimensionless velocity of the coating will increase as $1/\sqrt{E}$ with a decrease in elasticity modulus, and increase like $\eta^{-0.914}$ with a reduction of the loss tangent.

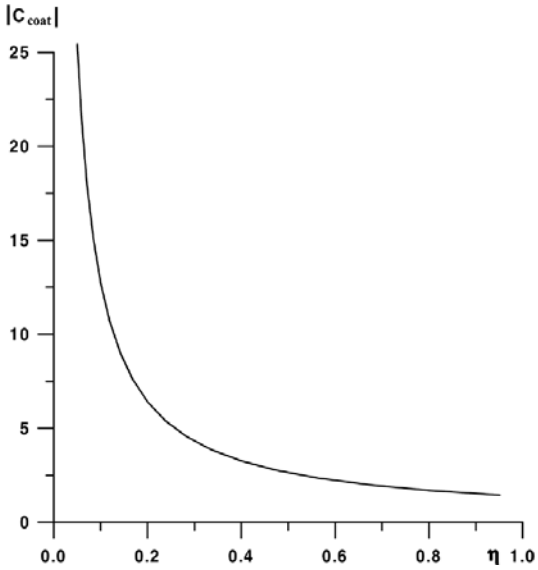

Fig. 12 Dependence of $|C_{coat}|$ on the loss tangent

From Eqs. (4) and (5), the amplitude of the coating deformation at the first resonance frequency is obtained as (for the stationary regime);

$$|\zeta_{stat}| \approx \frac{2}{\pi}\frac{PH}{E}\frac{|C_{coat}|}{(1+\eta^2)^{-1/4}}$$

Therefore, $|\zeta_{stat}|$ is proportional to $1/E$, with $v^+_{coat,stat}$ being proportional to $1/\sqrt{E}$. Such a difference between dependences of $v^+_{coat,stat}$ and $|\zeta_{stat}|$ on E leads to the fact that "hard" coatings (with large E) can have relatively higher velocity of surface motion compared to the deformation amplitude. This interesting fact can have an important application for the theoretical analysis of compliant coating operation. It can be assumed that the amplitude of coating deformation is low enough to be neglected ($|\zeta^+ < 1|$); however, the velocity of surface motion is not equivalent to zero, and it can be compared with vertical velocity fluctuations of the flow. Thus, one can completely obviate the difficulties associated with the realization of the boundary conditions on a moving wall (Benjamin, 1960).

The effective interaction between a compliant coating with turbulent flow depends not only on the velocity of the coating surface, but also on the width of the frequency bandwidth of the interaction, shown in Fig. 13. Here, the frequency bandwidth of the first resonance is determined at the level $l = 0.708$ (as in Fig. 9) from the maximum

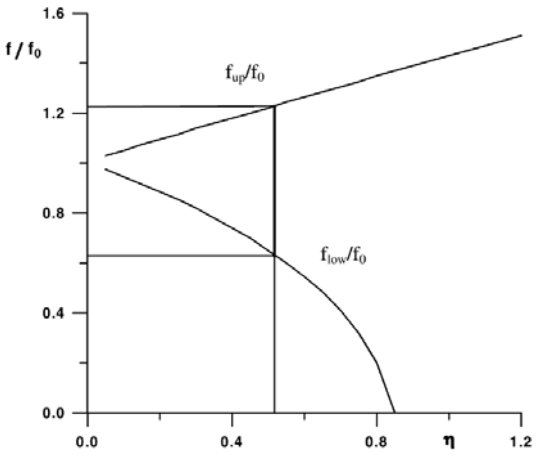

Fig. 13 The frequency bandwidth of the first resonance

deformation amplitude. For real coatings ($\eta <$ 0.5), this bandwidth is less than one octave and is drastically reduced with a decrease in the loss tangent.

In the previous work of authors' (Kulik et al., 2005), the properties of compliant coating, which are needed for drag reduction, have been derived. These properties, obtained from the analysis of the stationary regime of coating deformation, yield the dependences of coating thickness and modulus of elasticity on flow velocity. As noted above, however, a coating deformation is especially a non-stationary process and, therefore, the loss tangent plays a very important role in drag reduction. The increase in loss tangent has conflicting effects on the magnitude of coating deformation and drag reduction:

(1) positive effect: the relaxation process of forced oscillation becomes shorter (Fig. 9) and the frequency band of interaction becomes wider (Fig. 13);
(2) negative effect: the oscillation amplitude decreases (Fig. 8).

Therefore, care should be taken to find the optimal value of the loss tangent as well as other properties for maximum drag reduction, along with more detailed measurements in the turbulent boundary layer. This will be the main topic of the future researches.

6. Concluding Remarks

The transient response characteristics of a monolithic, hard compliant coating under 'modeled' turbulent pressure fluctuations were calculated in approximation of local deformation. The response of coating was analyzed with considerations of its inertial properties and limited duration of coherent harmonics action of pressure fluctuations. It is shown that a compliant coating interacts not with the whole spectrum of pressure fluctuations, but only with a frequency range near the first resonance. For sufficiently hard coatings, deformation amplitude becomes smaller than the thickness of viscous sublayer, while surface velocity remains comparable to vertical velocity fluctuations of the flow. It was also found that the loss tangent plays mutually conflicting roles on the magnitude of coating deformation and drag reduction. Consequently, it is envisaged that an optimal range for the loss tangent would be present for given specific flow conditions.

Acknowledgments

This research was sponsored by the Ministry of Commerce, Industry and Energy, Korea under the project PN00770 and by the ERC program (Advanced Ship Engineering Research Center) of MOST/KOSEF (grant #: R11-2002-104-05002-0)

References

Benjamin, T. B., 1960, "Effects of a Flexible Boundary on Hydrodynamic Stability," *Journal of Fluid Mechanics*, Vol. 9, pp. 513～532.

Blick, E. F. and Walters, R. R., 1968, "Turbulent Boundary-layer Characteristics of Compliant Surfaces," *Journal of Aircraft*, Vol. 5, pp. 11～16.

Bushnell, D. M., Hefner, J. N. and Ash, R. L., 1977, "Effect of Compliant wall Motion on Turbulent Boundary Layers," *Physics of Fluids*, Vol. 20, No. 10, Part II, pp. S31～S48.

Choi, K. -S., Yang, X., Clayton, B. R., Glover, E. J., Atlar, M., Semenov, B. N. and Kulik, V. M., 1997, "Turbulent Drag Reduction Using Compliant Surfaces," *Proceedings of. Royal Society of London A.*, Vol. 453, pp. 2229～2240.

Dixon, A. E., Lucey, A. D. and Carpenter, P. W., 1994, "The Optimization of Viscoelastic Compliant walls for Transition Delay," *AIAA Journal*, Vol. 32, pp. 256～267.

Duncan, J. H., 1986, "The Response of an Incompressible, Viscoelastic Coating to Pressure Fluctuations in a Turbulent Boundary Layer," *Journal of Fluid Mechanics*, Vol. 171, pp. 339～363.

Duncan, J. H., Waxman, A. M. and Tulin, M. P., 1985, "The Dynamics of Waves at the Interface Between a Biscoelastic Coating and a Fluid Flow," *Journal of Fluid Mechanics*, Vol. 158, pp. 177～197.

Fisher, M. C., Weinstein, L. M., Ash, R. L. and Bushnell, D. M., 1975, "Compliant Wall-Turbulent Skin-Friction Reduction Research," *AIAA Paper*, No. 75-833.

Gad-el-Hak, M., 1986, "The Response of Elastic and Viscoelastic Surfaces to a Turbulent Boundary Layer," *Journal of Applied Mechanics*, Vol. 53, pp. 206～212.

Gad-el-Hak, M., 1996, "Compliant Coatings : a Decade of Progress," *Applied Mechanics Review*, Vol. 49, No. 10, part 2, pp. S1～S11.

Gaster, M., 1988, "Is the dolphin a Red Herring?" In : Turbulence Management and Relaminarisation, eds. H.W. Liepmann and R. Narasimha, Springer-Verlag, pp. 285～304.

Kozlov, L. F., Tsyganyuk, A.I. and Babenko, V. V., 1985, "Formation of Turbulence in Shear Flows," *Kiev*, p. 284.

Kraichnan, R. H., 1956, "Pressure Fluctuations in Turbulent Flow Over a Flat Plate," *Journal of Acoustical Society of America*, Vol. 28, No. 3, pp. 378～390.

Kramer, M. O., 1957, "Boundary Layer Stabilization by Distributed Damping," *Journal of the Aeronautical Science*, Vol. 24, No. 6, pp. 459～460.

Kramer, M. O., 1960, "Boundary Layer Stabilization by Distributed Damping," *Journal of American Society of Naval Engineers*, 1962, Vol. 72, pp. 25～33.

Kulik, V. M., 2000, "Aging of Compliant Coatings," *Journal of Engineering Physics*, Vol. 73, No. 5, pp. 1088～1092.

Kulik, V. M., Poguda, I. S. and Semenov, B. N., 1991, "Experimental Investigation of One-Layer Viscoelastic Coating Action on Turbulent Friction and wall Pressure Fluctuations," In : Recent Develop. in Turbulence Manag., ed. K.-S. Choi, Kluwer, pp. 263～289

Kulik, V. M., Rodyakin, S. V., Lee, I. and Chun, H. H., 2005, "Deformation of a Viscoelastic Coating under the Action of Convective Pressure Fluctuations," *Experiments in Fluids*, Vol. 38, No. 5, pp. 648～655

Lee, T., Fisher, M. and Schwarz, W. H., 1993, "Investigation of the Stable Interaction of a Passive Compliant Surface with a Turbulent Boundary Layer," *Journal of Fluid Mechanics*, Vol. 257, pp. 373～401.

Lissaman, P. B. S. and Harris, G. L., 1969, "Turbulent skin friction on compliant surfaces," AIAA Paper No. 69-164.

Russell, S. J., 1998, "Measured wall Pressure Signatures of Turbulence Producing Structures," *Proceedings of the 1st International Symposium on Seawater Drag Reduction*, Newport, USA, pp. 63～71.

Semenov, B. N., 1991, "On Conditions of Modeling and Choice of Viscoelastic Coatings for Drag Reduction," *Recent Developments in Turbulence Management*, Kluwer, pp. 241～262.

Semenov, B. N., 1996, "Analysis of four Types of Viscoelastic Coatings for Turbulent Drag Reduction," In : *Emerging Techniques in Drag Reduction*, MEP, pp. 187～206.

Semenov, B. N. and Semenova, A. V., 1988, "Recent Developments in Interference Analysis of Compliant Boundary Action on Near-wall Turbulence," *Proceedings of the 1st International Symposium on Seawater Drag Reduction*, Newport, USA, pp. 189～195.

Spalart, P. R., 1988, "Direct Simulation of a Turbulent Boundary Layer Up to R_θ=1410," *Journal of Fluid Mechanics*, Vol. 187, pp. 61～98.

Willmarth, W. W., 1975, "Structure of Turbulence in Boundary Layers," *Advances in Applied Mechanics*, Vol. 15, pp. 159～254.